

RESEARCH PAPER

Leaf rolling precedes stomatal closure in rice (*Oryza sativa*) under drought conditions

Xiaoxiao Wang^{ID}, Jianliang Huang^{ID}, Shaobing Peng^{ID} and Dongliang Xiong^{*ID}

National Key Laboratory of Crop Genetic Improvement, Hubei Hongshan Laboratory, MOA Key Laboratory of Crop Ecophysiology and Farming System in the Middle Reaches of the Yangtze River, College of Plant Science and Technology, Huazhong Agricultural University, Wuhan, Hubei 430070, China

* Correspondence: dlxiong@mail.hzau.edu.cn

Received 31 December 2022; Editorial decision 2 August 2023; Accepted 5 August 2023

Editor: John Lunn, MPI of Molecular Plant Physiology, Germany

Abstract

Leaf rolling is a physiological response to drought that may help to reduce water loss, but its significance as a contribution to drought tolerance is uncertain. We scored the leaf rolling of four rice genotypes along an experimental drought gradient using an improved cryo-microscopy method. Leaf water potential (Ψ_{leaf}), gas exchange, chlorophyll fluorescence, leaf hydraulic conductance, rehydration capacity, and the bulk turgor loss point were also analysed. During the drought process, stomatal conductance declined sharply to reduce water loss, and leaves rolled up before the stomata completely closed. The leaf water loss rate of rolled leaves was significantly reduced compared with artificially flattened leaves. The Ψ_{leaf} threshold of initial leaf rolling ranged from -1.95 to -1.04 MPa across genotypes. When a leaf rolled so that the leaf edges were touching, photosynthetic rate and stomatal conductance declined more than 80%. Across genotypes, leaf hydraulic conductance declined first, followed by gas exchange and chlorophyll fluorescence parameters. However, the Ψ_{leaf} threshold for a given functional trait decline differed significantly among genotypes, with the exception of leaf hydraulic conductance. Our results suggested that leaf rolling was mechanistically linked to drought avoidance and tolerance traits and might serve as a useful phenotypic trait for rice breeding in future drought scenarios.

Keywords: $^{13}\text{CO}_2$ labeling, drought tolerance, leaf rolling, stomatal conductance, water loss, water potential threshold.

Introduction

Climate change is projected to aggravate drought (Ault, 2020), which may cause global food insecurity. Rice, one of the most important crops in the world, consumes a large amount of water. Unlike many other crops, rice is typically planted in paddy fields and is extremely sensitive to soil drought (reviewed by Bernier *et al.*, 2008). Developing new rice cultivars with enhanced drought tolerance is therefore urgent. As widely discussed in the literature, the major challenge for drought

tolerance breeding in the post-genomic era is the ‘phenotyping bottleneck’ (Furbank and Tester, 2011; Yang *et al.*, 2020). Because leaf rolling can be visually scored in the field, it has been proposed as a critical drought tolerance indicator of rice in recent high-throughput phenotyping projects (Guo *et al.*, 2018; Jiang *et al.*, 2021). Indeed, many efforts have been made to score the leaf rolling under drought conditions by monitoring the overall leaf geometry changes using spectral analysis

and image processing techniques (Lu *et al.*, 2011; Baret *et al.*, 2018; Cal *et al.*, 2019; Jiang *et al.*, 2021). However, whether the leaf rolling score can be used to assess rice drought tolerance is largely unclear, nor is the link clear between the leaf rolling score and other well-known drought tolerance traits. For instance, a recent study argued that genetic variation of rice leaf rolling under drought is related to leaf morphology rather than the common drought tolerance traits (Cal *et al.*, 2019).

Following drought, a rice leaf shows tubular rolling where one side of the leaf wraps over the other. As the effective leaf area declines, rolling was suggested to decrease leaf transpiration through changes in leaf conductance and thus maintain leaf water potential (Ψ_{leaf}) under drought conditions (O'Toole *et al.*, 1979; Clarke, 1986). Another important effect of leaf rolling proposed in the literature is decreasing light absorption, thus potentially protecting photosystems from damage caused by excessive light under severe drought (reviewed by Ali *et al.*, 2022). In addition, the decreased radiation absorption can reduce high leaf temperature, an important factor that can cause leaf damage under drought (Saglam *et al.*, 2014). As mentioned in these studies, leaf rolling in grasses represents a dehydration avoidance mechanism for plants facing drought. However, some studies suggest that carbon starvation due to reduced carbon assimilation under drought conditions is an important cause of plant mortality (Sevanto *et al.*, 2014; Adams *et al.*, 2017). Surprisingly, empirical studies quantifying the effects of leaf rolling on transpiration rate and photosynthetic carbon gain during drought have been rare.

Plant drought tolerance is widely estimated by the water potential that induces a decline in key physiological processes (Tyree and Sperry, 1989; Nardini *et al.*, 2001; Brodribb *et al.*, 2003; John *et al.*, 2018; Wang *et al.*, 2018). The sequence of water potential thresholds for drought tolerance traits has been suggested to influence overall plant function under drought dramatically. Previous studies have compared some drought tolerance traits, but the leaf rolling score has not been included in most studies (Bartlett *et al.*, 2016; John *et al.*, 2018; Trueba *et al.*, 2019; Yao *et al.*, 2021). The response of leaf rolling score to soil and plant water potential was investigated in several early studies, but those studies included limited information on other well-established drought tolerance traits (O'Toole *et al.*, 1979; Clarke, 1986; Dingkuhn *et al.*, 1989, 1999). Stomatal closure, measured as percentage stomatal conductance (g_{sw}) decline, was frequently observed at sufficiently high leaf water potentials to prevent wilting and xylem cavitation (Brodribb *et al.*, 2003; Bartlett *et al.*, 2016). Nevertheless, leaf water can be lost via the cuticle and imperfectly closed stomata, quantified as minimum leaf conductance (g_{min}). The g_{min} values of cereals were confirmed to be higher compared with other species groups (Duursma *et al.*, 2019). Therefore, leaf rolling may be a strategy to prevent water loss from leaves after stomatal closure in cereals like rice, but, again, the links among leaf rolling, g_{sw} decline, and g_{min} have rarely been tested.

The basis for leaf rolling is small changes in cell turgor pressure, which then aggregate to a macroscopic shape change at the tissue and organ levels (Matschi *et al.*, 2020; Ali *et al.*, 2022). Previous biomimetic studies have suggested that the leaf rolling in grasses is mainly controlled by the turgor pressure of bulliform cells, a group of large fan-shaped epidermal cells (Alvarez *et al.*, 2008; Mader *et al.*, 2020). Interestingly, leaf water potential at cellular turgor loss (π_{tp}) is widely recognized as a predominant physiological determinant of plant drought tolerance (Baltzer *et al.*, 2008; Bartlett *et al.*, 2012; Blackman, 2018; Zhu *et al.*, 2018). Over the last decades, the links between π_{tp} and other drought tolerance parameters, mainly Ψ_{leaf} thresholds for the declines of hydraulic dysfunction, stomatal closure, and leaf hydraulic performance, have been studied extensively (Brodribb and Holbrook, 2003; Bartlett *et al.*, 2016; Farrell *et al.*, 2017; Sorek *et al.*, 2021). These drought tolerance traits were generally well coordinated, and some hypotheses have been proposed to explain the observed trait correlations (Scoffoni *et al.*, 2014; McAdam and Brodribb, 2016). From this point of view, there may be a mechanistic link between leaf rolling and plant drought tolerance. Therefore, leaf rolling may be both a drought avoidance trait and a drought tolerance trait in rice.

Here, we quantified Ψ_{leaf} thresholds for leaf rolling score, gas exchange, hydraulic parameters, and chlorophyll fluorescence parameters, along with water loss rate and turgor loss point estimations in four rice genotypes with different drought tolerance. We asked the following questions: (i) How much plant water loss can leaf rolling reduce during water stress? (ii) What are the relationships between drought tolerance traits and leaf rolling score (i.e. determining the sequence of their water potential thresholds)?

Materials and methods

Plant materials and drought treatment

Four rice genotypes, MR185, Gang64B, La110, and TD70, with different leaf rolling susceptibility were selected in our study. The selection was based on the order of occurrence of leaf rolling under successive field drought of a rice variety collection containing 240 genotypes as determined by Jiang *et al.* (2021). In their trial, leaves of MR185 rolled much earlier than those of the other three genotypes after the drought started. In our trial, rice seeds were germinated in a nursery. Three weeks after sowing, seedlings were transplanted into 4.0-liter plastic pots containing 2.8 kg commercial soil (Xinnong Soil Technology Co., Ltd, Zhenjiang, China) with a plant density of a sole seedling per pot and 40 pots prepared for each genotype. Plants were grown outdoors on the Huazhong Agricultural University campus (E114.33°, N30.50°), Wuhan, China. Fifteen days after transplantation, 5.0 g compound fertilizer (N: P₂O₅: K₂O=16:16:16%; Batian Ecological Engineering Co., Ltd, Shenzhen, China) was added to each pot. Diseases, pests, and weeds were strictly controlled over the experimental period. Plants were well watered before applying drought treatment.

To capture different leaf-rolling phases, half of the pots of each genotype (20 pots) were subjected to gradual drought events by stopping irrigation in batches from the 30th day to the 32nd day after transplantation

(15–25 tillers, depending on genotype, were produced in each pot). During the soil drought, gas exchange and $^{13}\text{CO}_2$ labeling experiments were conducted with plants of different leaf rolling status. After gas exchange measurement and labeling, the leaves were sampled immediately for leaf water potential estimation and rolling scoring. At the same period, the water loss curve, the water potential at the turgor loss point (π_{tp}), and the vulnerability curves of rehydration capacity (RC), photosystem II (PSII) maximum quantum yield (F_v/F_m), and leaf hydraulic conductance (K_{leaf}) were measured on well-watered plants. We conducted the K_{leaf} vulnerability curve from well-watered plants to avoid the biases caused by the native state of damage, osmotic adjustment, and so on, as frequently discussed in previous studies (Johnson *et al.*, 2020; Smith-Martin *et al.*, 2020). The measurements were conducted on leaves collected from at least 10 individuals for each trait except for the measurements of water loss and pressure–volume curves in which leaves were collected from four individuals. All measurements were conducted between 30 and 45 d after transplantation.

Leaf rolling score

Inspired by Franks and Farquhar (2007) and Matschi *et al.* (2020), we developed a cryo-microscopy method to capture the leaf rolling dynamics during drought. After leaf water potential was measured using a pressure chamber (PMS Instrument Company, Albany, OR, USA), several ~1 cm lengths of leaf segments were quickly sampled at the middle of leaves, and the samples were immersed into liquid nitrogen immediately (see Supplementary Fig. S1A–C). Then, the frozen samples were transferred to $1.2 \times 1.2 \times 1.2$ silicone molds and vertically fixed by adding a pre-cold tissue freezing kit (Leica Microsystems Inc., Wetzlar, Germany). The silicone molds were placed in a steel container filled with liquid nitrogen during the fixing process (Supplementary Fig. S1D). Frozen tissue samples were cut at -15°C by using a cryostat (CM1950, Leica Microsystems Inc., Wetzlar, Germany), and tissue sections of about 100 μm thickness were obtained and stuck on the pre-frozen slides. Microscopical images of leaf transections were captured using a miniature portable microscope (ontp, Weixing Electronic Technology Co., Ltd, Shenzhen, China) inside the cryostat chamber (Supplementary Fig. S1E, F). Images were imported into GetData Graph Digitizer 2.26 (<https://getdata-graph-digitizer-software.informer.com/>). The positions of leaf veins and the two edges of the leaf were manually identified after establishing the coordinates containing two vertical vectors, x and y , on images (Supplementary Fig. S1G). By modifying the equation developed by Sirault *et al.* (2015), the leaf rolling score was calculated as follows:

$$\text{Rolling score} = \frac{\text{Transection perimeter}}{\text{Minimum outer convex hull perimeter}}$$

Transection perimeter, twice the total distances between two adjacent coordinate points, is the exposed perimeter when the leaf is flat. The minimum outer convex hull perimeter is the exposed perimeter of the transection. The estimation of transection perimeter and minimum outer convex hull perimeter was conducted using Python 3.6 (<https://www.python.org>; Supplementary Fig. S2).

Water loss curves

Water loss curves were obtained using artificial flattening of leaves and natural rolling of leaves in parallel to quantify the role of leaf rolling in preventing water loss during dehydration. Newly expanded leaves were sampled from four individuals at dawn for each genotype and rehydrated for 1 h in the lab. For the artificial flattening treatment, the leaves were fixed using pre-weighed homemade clips to keep the blades flat

during dehydration. Leaf segments (12 cm in length) were cut from the middle of sampled leaves, and two cut ends were sealed with melted candle wax immediately to minimize water loss from the wound. Samples were weighed quickly using an electronic balance (± 0.01 mg; Mettler MS205DU, Mettler-Toledo GmbH, Greifensee, Switzerland). Then the samples were hung in a foam box, awaiting subsequent weighing. Leaf samples were dried in an 80°C oven for 3 d after weighing. The leaf relative water content (RWC) was calculated as follows:

$$\text{RWC} = \frac{W_i - W_{\text{dr}}}{W_{\text{sa}} - W_{\text{dr}}}$$

where W_i is the leaf weight at time i during the measurement, and W_{dr} and W_{sa} are the dry weight and water-saturated weight of the leaves.

Gas exchange measurements

An open-flow infrared gas analysis system, LI-6800 (LI-COR Inc., Lincoln, NE, USA) with an integrated chlorophyll fluorescence leaf chamber (LI-6800-01, LI-COR Inc.), was used to measure gas exchange and chlorophyll fluorescence simultaneously. Inside the leaf chamber, the sample CO_2 concentration, light intensity, and flow rate were set to $400 \mu\text{mol mol}^{-1}$, $1200 \mu\text{mol photons m}^{-2} \text{s}^{-1}$ and $500 \mu\text{mol s}^{-1}$, respectively. Measurements were made outdoors between 09.00 h and 12.00 h, and rolled leaves were artificially flattened before placing in the leaf chamber. Once the CO_2 and H_2O concentrations in the gas exchange system reached stable states (typically, 30–60 s after clamping the chamber), the gas exchange was recorded. After the gas exchange was recorded, a saturating pulse (100 Hz ; approximately $10\,000 \text{ mmol photons m}^{-2} \text{s}^{-1}$) was applied. Values of steady-state fluorescence (F_s) and maximum fluorescence (F_m') in light conditions, and the actual photochemical efficiency of photosystem II ($\Phi_{\text{PSII}} = (F_m' - F_s)/F_m'$) were recorded. Then Ψ_{leaf} was measured using a pressure chamber. The mesophyll conductance of CO_2 (g_m) was calculated based on the method described by Harley *et al.* (1992), as follows:

$$g_m = \frac{A}{C_i - \frac{\Gamma^* ((\text{ETR} + 8(A + R_d))}{\text{ETR} - 4(A + R_d)}}$$

where A is the net photosynthetic rate, C_i is intercellular CO_2 concentration, ETR is the electron transport rate recorded in the LI-6800 instrument, Γ^* represents the CO_2 compensation point in the absence of respiration, and R_d is the day respiration rate. Typical values of $40 \mu\text{mol mol}^{-1}$ and $0.5 \mu\text{mol m}^{-2} \text{s}^{-1}$ were used for Γ^* and R_d , respectively (Hermida-Carrera *et al.*, 2016).

$^{13}\text{CO}_2$ labeling

To evaluate the influence of leaf rolling on carbon assimilation, 12 plants of each genotype with different leaf-rolling phases were labeled. Plants were sealed into transparent cylindrical chambers (18 cm diameter \times 60 cm height; shown in Fig. 4) and provided ($1.5 \text{ liters min}^{-1}$) with air for at least 30 min prior to switching to $400 \text{ ppm } ^{13}\text{CO}_2$ (99 atom%) replaced air (78% N_2 , 21% O_2 , and $400 \text{ ppm } ^{13}\text{CO}_2$; Niuruide Gas Co., Ltd, Wuhan, China). Gas entered the chambers through the inlet near the bottom and flowed out via the outlet near the top, and the gas flows were controlled using pre-calibrated flow controllers (FMA 5400A/5500A, Omega Engineering, Inc., Norwalk, CT, USA). The outflowing gas was introduced into the 0.1% NaOH solution to avoid potential ambient $^{13}\text{CO}_2$ pollution. Leaves were sampled after 10 min of labeling, and the samples were immediately immersed in liquid nitrogen for subsequent measurement of ^{13}C abundance. Leaf water potentials were measured

using other leaves of the same tiller. The frozen inactivated leaf samples were dried at 80 °C and ground to fine powder before the ^{13}C abundance was measured using a stable isotope ratio mass spectrometer (Isoprime 100, Elementar Trading Co., Ltd, Hanau, Germany).

Water status thresholds for loss of photosystem II maximum quantum yield and rehydration capacity

The maximum quantum yield of PSII was estimated as variable fluorescence (F_v)/maximum fluorescence (F_m), and F_v was calculated as F_m minus minimum fluorescence (F_0). Chlorophyll fluorescence was measured using a pulse-modulated fluorometer (Junior-PAM, Heinz Walz GmbH, Effeltrich, Germany). An intensity of 9200 $\mu\text{mol photons m}^{-2} \text{s}^{-1}$, from a blue light-emitting diode (445 nm; 20 Hz), was taken as the saturation pulse to estimate F_m and F_v . More than 30 leaves were sampled from 15 individuals per genotype and hydrated in darkness for 2 h to avoid non-photochemical acute photoinhibition. Then the leaves were bench-dehydrated to a range of dehydration states. Leaves were weighed after the chlorophyll fluorescence measurement to estimate relative water content (RWC), and the vulnerability curves of F_v/F_m were plotted as F_v/F_m against RWC.

In the present study, the rehydration capacity (RC) was also estimated according to John et al. (2018). After the F_v/F_m measurement, the dehydrated leaves stood in deionized water to recover for 10 h before weighing. Then, leaves were dried at 80 °C for 3 d to estimate their dry weights. RC was calculated as the ratio of rehydrated leaf water content to saturated leaf water content:

$$\text{RC} = \frac{W_{\text{re}} - W_{\text{dr}}}{W_{\text{sa}} - W_{\text{dr}}}$$

where W_{re} , W_{dr} , and W_{sa} are the weights of rehydrated, dry, and saturated leaves. The vulnerability curves of RC were established by plotting RC against the RWC of dehydrated leaves.

Vulnerability of leaf hydraulic conductance to water-potential decline

The evaporative flux method was adopted to measure the leaf hydraulic conductance (K_{leaf}), which is the ratio of steady-state flow rate (E , $\text{mmol m}^{-2} \text{s}^{-1}$) to the water potential driving force ($\Delta\Psi_{\text{leaf}}$, MPa; Sack and Scoffoni, 2012). The $\Delta\Psi_{\text{leaf}}$ was estimated as the difference between the potential of water at atmospheric pressure entering the petiole (i.e. 0 MPa for pure water) and the steady state Ψ_{leaf} (Ψ_{final}) at the end of the measurement. About 24–40 tillers were sampled at dawn from at least 15 pots per genotype and hydrated over 1 h in the lab. Before the K_{leaf} measurement was made, tillers were bench-dehydrated to a range of Ψ_{leaf} values (−3.0~−0.1 MPa) in the lab (air temperature of 26 ± 2 °C, and relative humidity of $40 \pm 10\%$ over the experimental period). The newly matured leaf with a 2 cm sheath was cut from the tiller under airless distilled water and then rapidly connected to silicone tubing under water to prevent air entering the system. The adjacent leaf was collected to determine the initial water potential (Ψ_{initial}). The other end of the tubing was connected to a water source on an electronic balance (± 0.01 mg; Mettler MS205DU, Mettler-Toledo GmbH, Greifensee, Switzerland) that logged data every 3 s to a computer to calculate E . The leaves were put on the net with the adaxial surface upwards and were irradiated by a lamp (light intensity at leaf level $\sim 1000 \mu\text{mol photons m}^{-2} \text{s}^{-1}$, 600 W, Weichuang Electronic Technology Co. Ltd, Wuhan, China). A box fan under the net was used to minimize the boundary resistance (wind speed at leaf level about 1 m s^{-1}). The water flow rate into the leaf was recorded until it was stable for at least 15 min, and a thermocouple determined the

leaf temperature once the stable states were achieved. Measurements were discarded if the flow rate failed to stabilize or suddenly changed, and the criteria for stabilizations are described in our previous study (Wang et al., 2022). The leaf was quickly removed from the tubing, the sheath was dabbed dry, and the leaf was equilibrated in the bag for at least 20 min before measuring the Ψ_{final} . K_{leaf} was calculated as follows:

$$K_{\text{leaf}} = \frac{E}{(0 - \Psi_{\text{leaf}})}$$

K_{leaf} values were normalized to those at 25 °C leaf temperature, considering that water viscosity varied with temperature (Yang and Tyree, 1993). During the measurement, dehydrated leaves may recover their leaf water potential before reaching a stable state, such that Ψ_{final} is less negative than the Ψ_{leaf} before K_{leaf} measurement (Ψ_{initial}), or, alternatively, the transpiration rate may be sufficient for Ψ_{final} to be driven lower than Ψ_{initial} (Scoffoni et al., 2011). To construct K_{leaf} vulnerability curves, the K_{leaf} was, therefore, plotted against whichever was lowest, Ψ_{initial} or Ψ_{final} (see Scoffoni et al., 2011).

Turgor loss point estimation

Tillers were sampled from four individuals per genotype in the early morning and fully hydrated for 1 h in darkness. Pressure–volume curve parameters were determined by squeezing water out of the leaf using a pressure chamber to achieve different leaf water potential and weighing. The turgor loss point was calculated following the method of L. Sack, J. Pasquet-Kok, and M. Bartlett (<https://prometheus-protocols.net/function/water-relations/pressure-volume-curves/leaf-pressure-volume-curve-parameters/>).

Data analysis

Segmented regression, conducted in the R package ‘segmented’ (Muggeo, 2008), was used to separate the phases in plots of rolling score against Ψ_{leaf} . The vulnerability curves, including A , g_{sw} , g_m , K_{leaf} , and Φ_{PSII} against Ψ_{leaf} and RC and F_v/F_m against RWC, were fitted using Weibull functions in the R package ‘fitplc’ (Duursma and Choat, 2017). The confidence intervals of the vulnerability curves were estimated using bootstrap methods in the R package ‘fitplc’. The thresholds calculated as RWC were converted to Ψ_{leaf} using the conversion factors estimated from Ψ_{leaf} versus RWC curves (Supplementary Fig. S3). The slope and intercept of water loss curves between artificially flattened and naturally rolled leaves were compared using the R package ‘simba’. Except for special notes, analyses and plotting were performed in R 4.1.2 (<https://cran.r-project.org>). It should be noted that this study has two types of droughts: *in situ* soil drought and bench dehydration with excised tillers. Excised tissue lacks connections to the root system and neighboring tillers, which may influence water supply and hormone activity, potentially leading to drought responses for some traits that differ from their responses to *in situ* drought. The current study estimated the responses of leaf water loss rate, rehydration capacity, and the maximum quantum yield of the PSII to drought based on the bench dehydration method. Moreover, different water potentials in constructing K_{leaf} vulnerability curves were also created by bench dehydration.

Results

The effects of leaf rolling on leaf water conservation

The water loss curves of artificially flattened and naturally rolled leaves were compared. In all the genotypes, leaf RWC

decreased curvilinearly with time after removal from tillers (Fig. 1). Rolled leaves had a significantly decreased water loss rate compared with the flattened leaves, resulting in a continuous increase in the RWC differences between artificially flattened and naturally rolled leaves over a period of 50 min. As the response was multiphasic with a nearly linear relationship between the RWC and time at the late stage, linear regressions were plotted, and the slopes were calculated to represent the water loss rate. In all the genotypes, linear regression slopes significantly differed between artificially flattened and naturally rolled leaves. The dynamics of stomatal conductance and leaf rolling score during soil drought are presented in Fig. 2. There were differences observed in sensitivities of g_{sw} to Ψ_{leaf} decline among genotypes. The Ψ_{leaf} threshold of the 50% loss in g_{sw} was -1.31 , -1.44 , -1.56 , and -1.84 MPa for MR185, Gang64B, La110, and TD70, respectively. The Ψ_{leaf} threshold of the 80% loss in g_{sw} was -1.72 , -1.49 , -2.07 , and -2.30 MPa for MR185, Gang64B, La110, and TD70, respectively. The segmented linear function was selected to separate the phases of the correlations of leaf rolling score and Ψ_{leaf} in the four genotypes, which

well conformed to the morphological dynamics of transection in the captured images (Supplementary Fig. S4). With Ψ_{leaf} decline, the leaf rolling score showed a plateau until a breakpoint appeared and then linearly increased. The water potential at the breakpoint is referred to as the leaf water potential threshold of initial leaf rolling and had values of -1.04 , -1.26 , -1.64 , and -1.95 MPa for MR185, Gang64B, La110, and TD70, respectively. The Ψ_{leaf} at leaf rolling score 2 varied from -2.75 MPa for TD70 to -1.80 MPa for MR185 (Fig. 2). At the Ψ_{leaf} threshold of rolling score 2, g_{sw} had declined more than 80% in all genotypes.

The relationships between leaf rolling and photosynthetic capacity

The photosynthetic rate (A) measured by infrared gas analysis declined with Ψ_{leaf} and the Ψ_{leaf} response curves of A differed in shape among genotypes (Fig. 3A; Supplementary Fig. S5A). The Ψ_{leaf} threshold for the 50% loss of A was -1.44 , -1.52 , -1.95 , and -2.34 MPa for Gang64B, MR185, La110, and TD70, respectively. The responses of mesophyll conductance

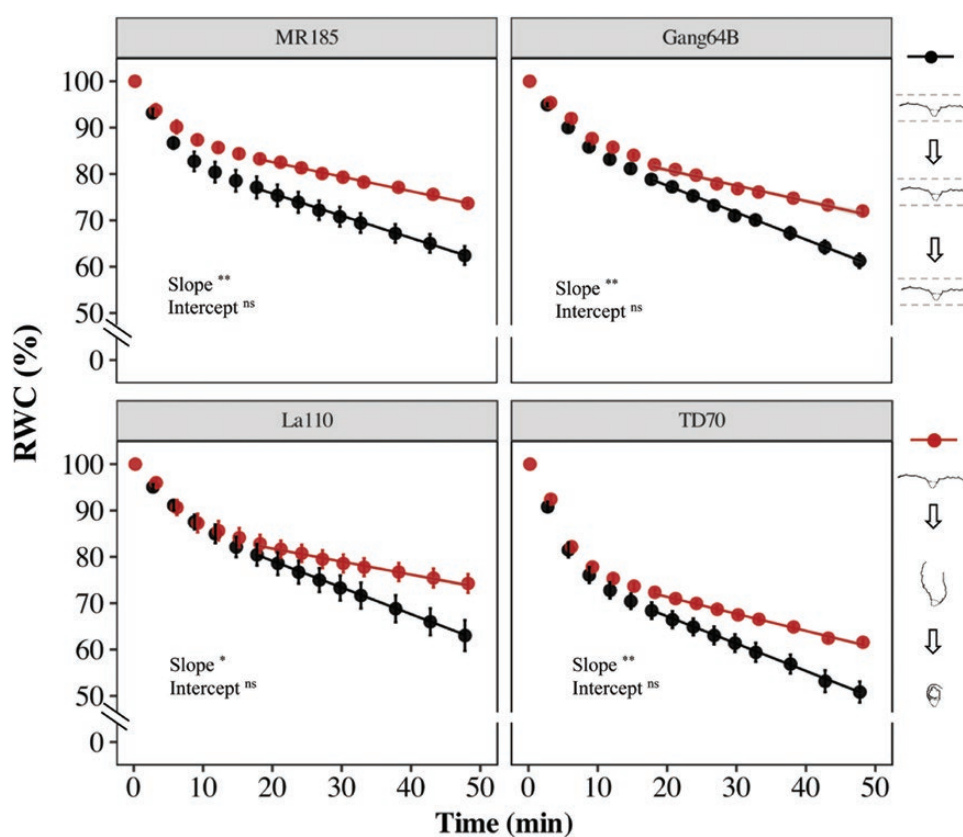


Fig. 1. Water loss curves of artificially flattened and naturally rolled rice leaves. The red and black circles represent the means of leaf relative water content (RWC) for naturally rolled and artificially flattened leaves, respectively. The red and black lines were fitted by a linear model, and the slopes and intercepts of lines were compared. Morphological changes in leaf cross-sections over the initial 18-min dehydration are shown on the right. The means (\pm SE) are shown ($n=4$). The significance of differences for slopes and intercepts was compared in R package 'simba' using randomization tests. * $P<0.05$; ** $P<0.01$.

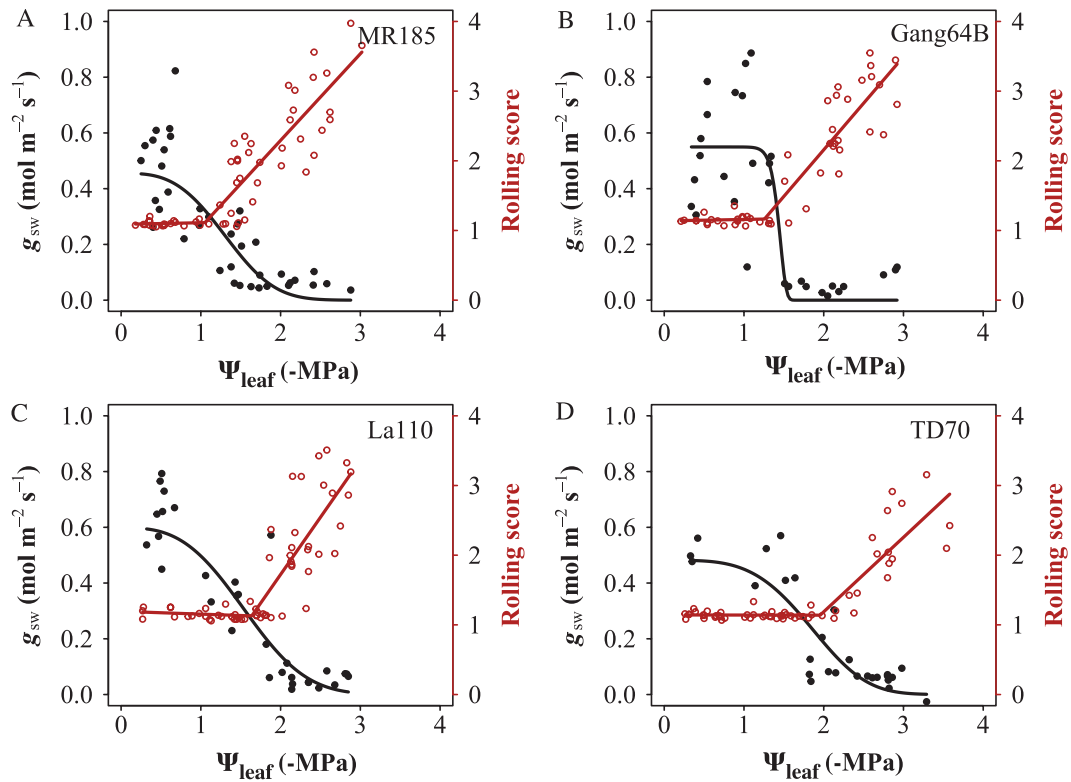


Fig. 2. The correlations of stomatal conductance (g_{sw}) and leaf rolling score with leaf water potential (Ψ_{leaf}). Black and red circles represent g_{sw} and leaf rolling scores, respectively. The correlations of g_{sw} with Ψ_{leaf} were fitted using the Weibull function, and the correlations between leaf rolling score and Ψ_{leaf} were estimated using the linear segmented regression method.

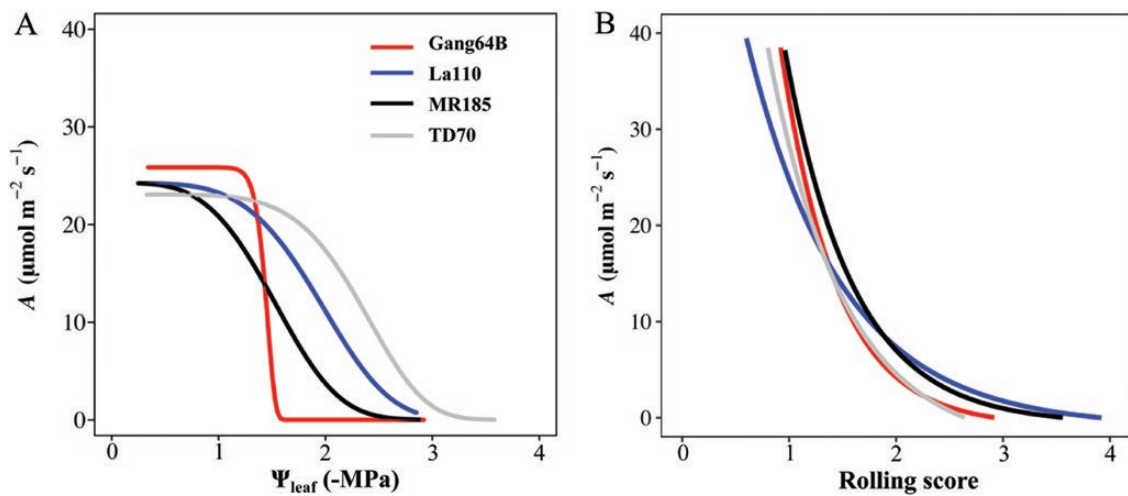


Fig. 3. Responses of photosynthetic rate (A) to leaf water potential (Ψ_{leaf} , A) and leaf rolling score (B). The response curves of A to Ψ_{leaf} were fitted by the Weibull function, and curves of A to rolling score were fitted using an exponential model.

(g_m) to Ψ_{leaf} decline were similar in shape to the responses of A (Supplementary Fig. S5B). Although the actual photochemical efficiency of PSII (Φ_{PSII}) declined with leaf dehydration, the threshold of Ψ_{leaf} for Φ_{PSII} decline was more negative compared with A (Supplementary Fig. S5C). Over the leaf dehydration, the decline of A was tightly correlated with the decreases

of g_{sw} , g_m , and Φ_{PSII} (Supplementary Fig. S6). Interestingly, A responded to the rolling score exponentially, and the response curves were similar among genotypes (Fig. 3B). Once the leaf rolling score achieved 2 (leaf edges touching), A was lower than $10 \mu\text{mol m}^{-2} \text{s}^{-1}$, and then A decreased smoothly with continuous leaf rolling.

The leaf photosynthetic capacity estimated by ^{13}C labeling agreed with gas exchange measured by infrared gas analysis. The ^{13}C relative abundance of labeled leaves decreased with decreasing Ψ_{leaf} in all genotypes (Fig. 4; Supplementary Fig. S7). But under the moderate drought ($\Psi_{\text{leaf}} -1.9$ to -1.3 MPa), TD70 and La110 with flat leaves tended to have higher leaf ^{13}C relative abundance than Gang64B and MR185 with rolled leaves. Moreover, in Fig. 4 it is clearly seen that plants and leaf transection morphologies were well coordinated, which confirmed that the leaf rolling degree could be obtained with the cryo-microscopy method.

Leaf rolling within the sequences of drought-induced functional decline

Along with leaf rolling score and photosynthetic performances, the vulnerability curves of leaf hydraulic conductance (K_{leaf}), leaf rehydration capacity (RC), and the maximum quantum yield of PSII (F_v/F_m) to leaf dehydration were also estimated in this study (Supplementary Figs S5D, S8). Further, we calculated leaf water potential thresholds inducing 50% and 80% losses of the leaf function based on the fitted Weibull functions for each trait. Function loss threshold sequences are shown in Fig. 5 and Supplementary Fig. S9. Across genotypes, K_{leaf} declined first, followed by gas exchange traits and chlorophyll fluorescence parameters (Supplementary Fig. S9). Leaves started rolling at π_{tip} before reaching the Ψ_{leaf} at 50% decline of A (A_{50}). A_{50} tended to be more negative than the Ψ_{leaf} at 50% loss of stomatal conductance ($g_{\text{sw}50}$) and be followed by Ψ_{leaf} at 50% loss of mesophyll conductance ($g_{\text{m}50}$) during leaf dehydration. However, the differences in these leaf water potential thresholds were only statistically significant for La110. In all genotypes, the leaf rolling score of 2 coincided with a 50% decline of Φ_{PSII} , and $\Phi_{\text{PSII}50}$ was lower than A_{50} except for La110. As the leaf water

potential thresholds for the 50% decline of F_v/F_m and RC were very low (lower than -10 MPa), we then calculated the leaf water potential thresholds for a 10% decline of those traits (F_v/F_{m10} , RC_{10}). F_v/F_{m10} was -4.86 ± 1.30 MPa which was more negative than the Ψ_{leaf} at rolling score 3 (Roll=3) and $\Phi_{\text{PSII}80}$. As a result, the F_v/F_{m10} was located at the end of the functional decline sequence (Fig. 5; Supplementary Fig. S9).

The sequences of leaf water potential thresholds for functional traits were similar among genotypes. However, the leaf water potential threshold for a given functional trait differed significantly among genotypes except for K_{leaf} (Fig. 5; Supplementary Fig. S9). The leaf water potential thresholds for most estimated traits were more negative in TD70 than in the other three genotypes, although the difference was not significant in g_{sw} , g_{m} , initial leaf rolling, and bulk turgor pressure loss. MR185 and Gang64B had high Ψ_{leaf} thresholds for all traits except for RC and F_v/F_m , and La110 had relatively negative Ψ_{leaf} thresholds for gas exchange traits.

Discussion

Leaf rolling reduces water loss

In higher plants, preventing water loss from transpiration by closing stomata is the initial response to drought (Bartlett *et al.*, 2016; Brodrribb *et al.*, 2020). In agreement, the g_{sw} of all the investigated rice genotypes declined rapidly as leaf water potential decreased under drought conditions. As observed in previous studies (Price *et al.*, 1997; Khowaja and Price, 2008; Cal *et al.*, 2019), the leaf water potential thresholds for stomatal closure varied greatly among rice genotypes, suggesting that genotype-specific management strategies should be developed to maximize water use efficiency. Interestingly, leaf rolling was initiated before the stomata fully closed in all the investigated

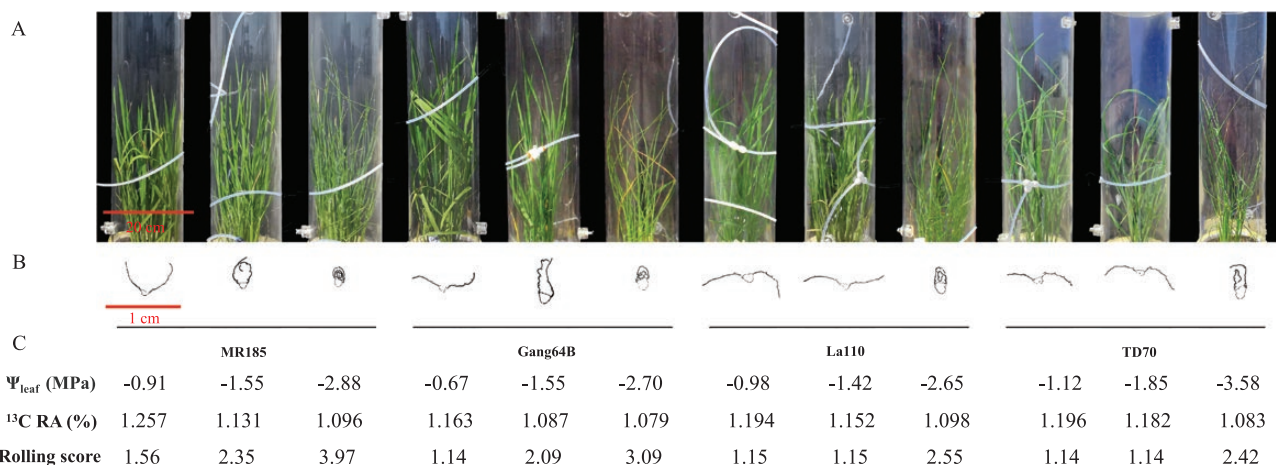


Fig. 4. The $^{13}\text{CO}_2$ labeling experiment. (A) Pot-grown rice plants were sealed in labeling chambers. (B) Monochrome images showing the binarized leaf middle transection of newly expanded leaves sampled after the labeling. (C) The values of leaf water potential (Ψ_{leaf}), ^{13}C relative abundance (RA), and rolling scores of the leaves shown in (B); the mean values of these traits are shown in Supplementary Fig. S7.

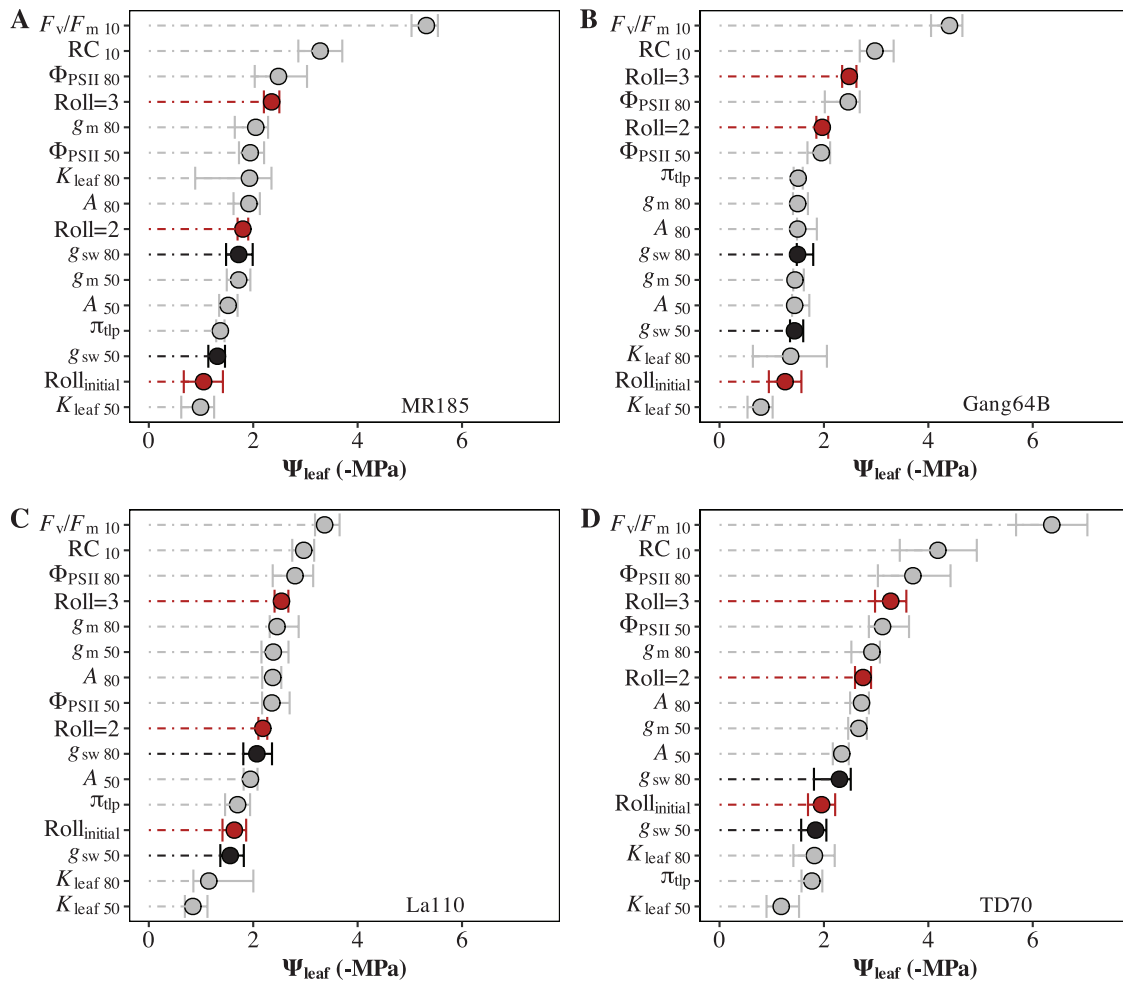


Fig. 5. The sequences of physiological responses to decreasing leaf water potential (Ψ_{leaf}). Roll_{initial}, the Ψ_{leaf} at initial leaf rolling; Roll=2, 3, the Ψ_{leaf} at leaf rolling score 2 and 3, respectively; g_{sw50} and g_{sw80} , the Ψ_{leaf} at 50% and 80% stomatal conductance decline, respectively; K_{leaf50} and K_{leaf80} , the Ψ_{leaf} at 50% and 80% leaf hydraulic conductance decline, respectively; π_{tlp} , the Ψ_{leaf} at leaf bulk turgor loss point; A_{50} and A_{80} , the Ψ_{leaf} at 50% and 80% photosynthetic rate loss, respectively; g_{m50} and g_{m80} , the Ψ_{leaf} at 50% and 80% mesophyll conductance loss, respectively; Φ_{PSII50} and Φ_{PSII80} , the Ψ_{leaf} at 50% and 80% loss of Φ_{PSII} , respectively; RC₁₀, the Ψ_{leaf} at 10% loss of rehydration capacity; F_v/F_{m10} , the Ψ_{leaf} at 10% loss of F_v/F_m . The bars are 95% confidence intervals of the estimated values.

genotypes, which suggests that leaf rolling might play a role in water conservation before the stomata close completely.

In the current study, we quantified the contribution of leaf rolling to the water loss rate by estimating the water loss curves of artificially flattened and naturally rolled leaves during dehydration. Water can be lost from stomata and continue escaping through the cuticle and by guard cell leakage after stomatal closure; the latter is commonly termed residual transpiration or minimum leaf transpiration (Duursma *et al.*, 2019). In principle, both stomatal transpiration and residual transpiration rates can be estimated from the water loss curve (Khowaja and Price, 2008). As shown in Fig. 1, water loss was very fast in the first phase of the curves. Therefore, the stomatal transpiration rate cannot be calculated robustly from the water loss curve with limited estimations in the current study. In addition, since stomatal movement is sensitive to leaf excision and environmental conditions, stomatal transpiration

likely differed significantly from reality. Leaf rolling significantly reduced the residual water loss for all the genotypes (Fig. 1). Notwithstanding, the measurement was insufficient to separate the leaf conductance and boundary-layer conductance. The reduced leaf transpiration rate of rolled leaves may predominately result from the decrease of boundary-layer conductance as the micro-environment inside the rolling space, including wind speed, humidity, and temperature, was changed (O’Toole *et al.*, 1979; Saglam *et al.*, 2014; Assmann and Jegla, 2016). As the leaf shape and environmental conditions around leaf surfaces significantly change when the leaf rolls up, stomatal and cuticular conductance adjustments are expected. Indeed, Bueno *et al.* (2019) revealed that minimum conductance was significantly affected by measuring temperature. Clearly, more effort should be made to understand how leaf rolling regulates water loss through stomatal pores and cuticles.

Carbon assimilation dramatically declined after rolling

Although leaf rolling can minimize water loss under drought, it potentially decreases carbon assimilation (Dingkuhn *et al.*, 1989; Corlett *et al.*, 1994). Indeed, carbon starvation was suggested to be one of the mechanisms underlying plant mortality under drought (McDowell *et al.*, 2008; Kono *et al.*, 2019), and many studies have attempted to clarify the relationship between carbon assimilation efficiency and drought tolerance (Bian *et al.*, 2019; Salmon *et al.*, 2020; Salvi *et al.*, 2021). In the current study, A declined in response to Ψ_{leaf} decrease, and Ψ_{leaf} thresholds of photosynthetic decline differed among rice genotypes. The reduced A was related to the decreased CO_2 supply capacity (both stomatal and mesophyll conductance to CO_2 , g_s and g_m) as well as biochemistry of photosynthesis (i.e. Φ_{PSII}). Agreeing with our previous study on rice, the decreases of g_s and g_m were faster than Φ_{PSII} (Supplementary Fig. S5; Wang *et al.*, 2018), suggesting that in drought A is predominantly limited by CO_2 supply capacity. Further correlation analysis also supported that A was mainly limited by g_s and g_m under drought (Supplementary Fig. S6). The genotype differences in the g_s versus Ψ_{leaf} relationship indicated that stomatal regulation of Ψ_{leaf} in rice might be described as falling along a classic isohydric–aniso-hydric continuum. According to the iso/aniso-hydric classification, isohydric behaviors are those in which g_{sw} declines rapidly to maintain Ψ_{leaf} relatively stable as environmental conditions change, whereas aniso-hydric behaviors keep stomata open, the resulting Ψ_{leaf} tracking environmental fluctuations in water availability. As shown in Fig. 2, stomata open for a long time enables the relatively aniso-hydric genotypes TD70 and La110 to assimilate more carbon during drought than the other two.

Photosynthesis declined exponentially with the leaf rolling score, and the leaf rolling score thresholds of photosynthesis showed no difference among genotypes (Fig. 3). As described in the ‘Materials and methods’, the leaves were forced to be flat when A was measured by infrared gas analysis; the decline of A was unlikely to be caused by the decline of the photosynthetic area. The exponential relationship was further supported by the *in situ* $^{13}\text{CO}_2$ labeling results (Fig. 4). Our result suggests that the relationship between A and the leaf rolling score should reflect a mechanistic link between leaf rolling and photosynthetic function. Leaf rolling score was previously used for selection in rice drought breeding programs but was discontinued due to its lack of correlation with grain yield (see O’Toole *et al.*, 1979; Price *et al.*, 1997). Here we highlight the need to explore more detailed aspects of leaf rolling under drought conditions that could potentially be linked to yield beyond the traditional approach of maximizing leaf rolling score under severe drought stress.

The Ψ_{leaf} sequence of leaf functional declines

Thresholds for functional decline during dehydration in leaf water potential have been widely investigated across species

(Bartlett *et al.*, 2016; John *et al.*, 2018; Trueba *et al.*, 2019; Yao *et al.*, 2021). In the current study, we provided an empirically based sequence of functional declines in response to leaf water potential in rice. The sequence of rice Ψ_{leaf} thresholds for stomatal closure and hydraulic decline differs from the sequence across species. In previous studies (Bartlett *et al.*, 2016; Trueba *et al.*, 2019), $g_{\text{sw}50}$ was lower than $K_{\text{leaf}50}$ across species, but the K_{leaf} decline occurred significantly before the decline of g_{sw} in rice. Our result is consistent with recent studies (Tombesi *et al.*, 2015; Rodriguez-Dominguez *et al.*, 2016; Wang *et al.*, 2018) in which the decline of K_{leaf} is suggested to trigger rapid stomatal closure in response to drought. Similar to the findings across species, π_{tip} coincided with $g_{\text{sw}50}$, supporting that significant stomatal closure acts to prevent mesophyll wilt in some species (Brodrribb *et al.*, 2003; Bartlett *et al.*, 2016; Farrell *et al.*, 2017). Moreover, the decline in PSII photochemistry occurred at lower water potentials than g_{sw} , A , K_{leaf} , and bulk turgor pressure loss. The leaf water potential threshold of PSII efficiency decline was more negative in darkness than in light, which agreed with the previous results (Flexas *et al.*, 2002; Souza *et al.*, 2004).

In the current study, we found that leaf rolling score is a key indicator of drought stress. When stomatal and leaf hydraulic conductance declined by more than 50% of their value, leaves lost turgor pressure and rolled. At the same time, leaf rolling decreased leaf water loss and thus delayed leaf water potential decline, potentially protecting leaf functions from irreversible leaf damage, such as rehydration capacity and F_v/F_m declines (John *et al.*, 2018; Lopez-Pozo *et al.*, 2019; Trueba *et al.*, 2019). Our observations suggest that the leaf rolling score can be used as a drought avoidance parameter as well as a drought tolerance indicator. Leaf rolling in grasses is physically caused by the volume changes of the bulliform cells, a type of specialized epidermal cell, and the cell volume directly relates to cell turgor pressure (Arber, 2010). The reduction in bulliform cell volumes can be caused by direct water loss through the bulliform cuticle or indirect water loss through guard cells, another type of specialized epidermal cell. Matschi *et al.* (2020) proposed that the higher water permeability of the bulliform cell cuticle compared with other epidermal cells contributes to the fast cell volume reduction of bulliform cells in maize. However, we found that the Ψ_{leaf} threshold of initial leaf rolling was very close to the π_{tip} of rice leaf (Fig. 5), suggesting that the cellular turgor pressure reduction may occur simultaneously in bulliform cells and mesophyll cells. It is worth noting that π_{tip} was estimated on leaves with water equilibrium, but water potential gradients inside leaves are expected in reality (Buckley *et al.*, 2017; Wong *et al.*, 2022). Future work is needed to clarify the regulation of bulliform cell turgor pressure during water stress. If the leaf rolling reflects the turgor pressure reduction of a leaf rather than the turgor pressure loss of the bulliform cells alone, it is not surprising that other physiological functions can be predicted using the leaf rolling score. As the transport of water and CO_2 molecules across

membranes and cell walls is tightly regulated by the turgor pressure of cells (summarized by [Hernandez-Hernandez *et al.*, 2020](#)), both g_m and K_{leaf} declined dramatically during leaf dehydration.

Further research is still needed to uncover the leaf rolling reflecting drought tolerance and the potential mechanisms behind it across a broader range of rice genotypes. We demonstrated that leaf rolling prevents leaf water loss during the late stage of stomatal closure with dehydration. Once the leaves rolled to the point of touching the edge, photosynthetic rate and stomatal conductance declined by over 80%. In all genotypes, the decline in leaf hydraulic conductance occurred first, and the leaf water potential thresholds for functional trait decline varied significantly among genotypes. It is noteworthy that we found a remarkable resemblance between the leaf water potential threshold of initial leaf rolling and the leaf turgor loss point across all genotypes, which suggests a strong correlation between bulliform cell turgor pressure, guard cell aperture, and bulk cell turgor pressure.

Supplementary data

The following supplementary data are available at [JXB online](#).

Fig. S1. Overview of the cryo-microscopy method to score the leaf rolling.

Fig. S2. Diagrams of the leaf rolling score estimation.

Fig. S3. The bulk cellular water relations.

Fig. S4. Binarized images showing typical leaf transection and their leaf rolling score under a range of leaf water potential.

Fig. S5. The vulnerability curves of leaf physiological traits to dehydration.

Fig. S6. The relationships between photosynthetic traits.

Fig. S7. The ^{13}C relative abundance of leaves with different leaf water potential.

Fig. S8. The responses of rehydration capacity and the maximum quantum yield of photosystem II to relative water content reduction.

Fig. S9. The genotypic variation of sequences of physiological responses to decreasing leaf water potential.

Acknowledgements

The authors thank Sheng Liang, Kangkang Zheng, Ya Zhang, and Meng Tian for their help in conducting measurements, Sicheng Liu for his help with calculating the convex hull perimeter, and Dr Junzhou Liu for his critical comments on the manuscript.

Author contributions

DX contributed to conceptualization and supervision. XW contributed to data collection. XW and DX contributed to data analysis. XW, JH, SP, and DX contributed to writing.

Conflict of interest

The authors declare that they have no conflict of interest.

Funding

This study was supported by the National Natural Science Foundation of China (No. 32022060) and the China Agriculture Research System (CARS-01-23).

Data availability

All relevant data can be found within the article and its supporting supplementary data.

References

- Adams HD, Zeppel MJB, Anderegg WRL, *et al.*** 2017. A multi-species synthesis of physiological mechanisms in drought-induced tree mortality. *Nature Ecology & Evolution* **1**, 1285–1291.
- Ali Z, Merrium S, Habib-ur-Rahman M, Hakeem S, Saddique MAB, Sher MA.** 2022. Wetting mechanism and morphological adaptation; leaf rolling enhancing atmospheric water acquisition in wheat crop—a review. *Environmental Science and Pollution Research* **29**, 30967–30985.
- Alvarez JM, Rocha JF, Machado SR.** 2008. Bulliform cells in *Loudetiopsis chrysothrix* (Nees) Conert and *Tristachya leiostachya* Nees (Poaceae): structure in relation to function. *Brazilian Archives of Biology and Technology* **51**, 113–119.
- Arber A.** 2010. The vegetative phase in grasses: the leaf. In: Arver A, ed. *The Gramineae: a study of cereal, bamboo and grass*. Cambridge: Cambridge University Press, 279–306.
- Assmann SM, Jegla T.** 2016. Guard cell sensory systems: recent insights on stomatal responses to light, abscisic acid, and CO₂. *Current Opinion in Plant Biology* **33**, 157–167.
- Ault TR.** 2020. On the essentials of drought in a changing climate. *Science* **368**, 256–260.
- Baltzer JL, Davies SJ, Bunyavejchewin S, Noor NSM.** 2008. The role of desiccation tolerance in determining tree species distributions along the Malay-Thai Peninsula. *Functional Ecology* **22**, 221–231.
- Baret F, Madec S, Irfan K, Lopez J, Comar A, Hemmerle M, Dutartre D, Praud S, Tixier MH.** 2018. Leaf-rolling in maize crops: from leaf scoring to canopy-level measurements for phenotyping. *Journal of Experimental Botany* **69**, 2705–2716.
- Bartlett MK, Klein T, Jansen S, Choat B, Sack L.** 2016. The correlations and sequence of plant stomatal, hydraulic, and wilting responses to drought. *Proceedings of the National Academy of Sciences, USA* **113**, 13098–13103.
- Bartlett MK, Scoffoni C, Sack L.** 2012. The determinants of leaf turgor loss point and prediction of drought tolerance of species and biomes: a global meta-analysis. *Ecology Letters* **15**, 393–405.
- Bernier J, Atlin GN, Serraj R, Kumar A, Spaner D.** 2008. Breeding upland rice for drought resistance. *Journal of the Science of Food and Agriculture* **88**, 927–939.
- Bian Z, Zhang X, Wang Y, Lu C.** 2019. Improving drought tolerance by altering the photosynthetic rate and stomatal aperture via green light in tomato (*Solanum lycopersicum* L.) seedlings under drought conditions. *Environmental and Experimental Botany* **167**, 103844.
- Blackman CJ.** 2018. Leaf turgor loss as a predictor of plant drought response strategies. *Tree Physiology* **38**, 655–657.
- Brodribb TJ, Holbrook NM.** 2003. Stomatal closure during leaf dehydration, correlation with other leaf physiological traits. *Plant Physiology* **132**, 2166–2173.

- Brodribb TJ, Holbrook NM, Edwards EJ, Gutierrez MV.** 2003. Relations between stomatal closure, leaf turgor and xylem vulnerability in eight tropical dry forest trees. *Plant, Cell & Environment* **26**, 443–450.
- Brodribb TJ, Susmilch F, McAdam SAM.** 2020. From reproduction to production, stomata are the master regulators. *The Plant Journal* **101**, 756–767.
- Buckley TN, John GP, Scoffoni C, Sack L.** 2017. The sites of evaporation within leaves. *Plant Physiology* **173**, 1763–1782.
- Bueno A, Alfarhan A, Arand K, Burghardt M, Deininger AC, Hedrich R, Leide J, Seufert P, Staiger S, Riederer M.** 2019. Effects of temperature on the cuticular transpiration barrier of two desert plants with water-spender and water-saver strategies. *Journal of Experimental Botany* **70**, 1613–1625.
- Cal AJ, Sanciangco M, Rebolledo MC, Luquet D, Torres RO, McNally KL, Henry A.** 2019. Leaf morphology, rather than plant water status, underlies genetic variation of rice leaf rolling under drought. *Plant, Cell & Environment* **42**, 1532–1544.
- Clarke JM.** 1986. Effect of leaf rolling on leaf water loss in *Triticum* spp. *Canadian Journal of Plant Science* **66**, 885–891.
- Corlett JE, Jones HG, Massacci A, Masojidek J.** 1994. Water deficit, leaf rolling and susceptibility to photoinhibition in field grown sorghum. *Physiologia Plantarum* **92**, 423–430.
- Dingkuhn M, Audebert AY, Jones MP, Etienne K, Sow A.** 1999. Control of stomatal conductance and leaf rolling in *O. sativa* and *O. glaberrima* upland rice. *Field Crops Research* **61**, 223–236.
- Dingkuhn M, Cruz R, O'Toole J, Drffling K.** 1989. Net photosynthesis, water use efficiency, leaf water potential and leaf rolling as affected by water deficit in tropical upland rice. *Australian Journal of Agricultural Research* **40**, 1171–1181.
- Duursma RA, Blackman CJ, Lopez R, Martin-StPaul NK, Cochard H, Medlyn BE.** 2019. On the minimum leaf conductance: its role in models of plant water use, and ecological and environmental controls. *New Phytologist* **221**, 693–705.
- Duursma RA, Choat B.** 2017. fitplr – an R package to fit hydraulic vulnerability curves. *Journal of Plant Hydraulics* **4**, e002.
- Farrell C, Szota C, Arndt SK.** 2017. Does the turgor loss point characterize drought response in dryland plants? *Plant, Cell & Environment* **40**, 1500–1511.
- Flexas J, Bota J, Escalona JM, Sampol B, Medrano H.** 2002. Effects of drought on photosynthesis in grapevines under field conditions: an evaluation of stomatal and mesophyll limitations. *Functional Plant Biology* **29**, 461–471.
- Franks PJ, Farquhar GD.** 2007. The mechanical diversity of stomata and its significance in gas-exchange control. *Plant Physiology* **143**, 78–87.
- Furbank RT, Tester M.** 2011. Phenomics – technologies to relieve the phenotyping bottleneck. *Trends in Plant Science* **16**, 635–644.
- Guo Z, Yang W, Chang Y, et al.** 2018. Genome-wide association studies of image traits reveal genetic architecture of drought resistance in rice. *Molecular Plant* **11**, 789–805.
- Harley PC, Loreto F, Di Marco G, Sharkey TD.** 1992. Theoretical considerations when estimating the mesophyll conductance to CO₂ flux by analysis of the response of photosynthesis to CO₂. *Plant Physiology* **98**, 1429–1436.
- Hermida-Carrera C, Kapralov MV, Galmes J.** 2016. Rubisco catalytic properties and temperature response in crops. *Plant Physiology* **171**, 2549–2561.
- Hernandez-Hernandez V, Benitez M, Boudaoud A.** 2020. Interplay between turgor pressure and plasmodesmata during plant development. *Journal of Experimental Botany* **71**, 768–777.
- Jiang Z, Tu H, Bai B, et al.** 2021. Combining UAV-RGB high-throughput field phenotyping and genome-wide association study to reveal genetic variation of rice germplasms in dynamic response to drought stress. *New Phytologist* **232**, 440–455.
- John GP, Henry C, Sack L.** 2018. Leaf rehydration capacity: associations with other indices of drought tolerance and environment. *Plant, Cell & Environment* **41**, 2638–2653.
- Johnson KM, Brodersen CR, Carins-Murphy MR, Choat B, Brodribb TJ.** 2020. Xylem embolism spreads by single-conduit events in three dry forest angiosperm stems. *Plant Physiology* **184**, 212–222.
- Khawaja FS, Price AH.** 2008. QTL mapping rolling, stomatal conductance and dimension traits of excised leaves in the BalaxAzucena recombinant inbred population of rice. *Field Crops Research* **106**, 248–257.
- Kono Y, Ishida A, Saiki ST, Yoshimura K, Dannoura M, Yazaki K, Kimura F, Yoshimura J, Aikawa SI.** 2019. Initial hydraulic failure followed by late-stage carbon starvation leads to drought-induced death in the tree *Trema orientalis*. *Communications Biology* **2**, 8.
- Lopez-Pozo M, Flexas J, Gulias J, et al.** 2019. A field portable method for the semi-quantitative estimation of dehydration tolerance of photosynthetic tissues across distantly related land plants. *Physiologia Plantarum* **167**, 540–555.
- Lu Y, Hao Z, Xie C, et al.** 2011. Large-scale screening for maize drought resistance using multiple selection criteria evaluated under water-stressed and well-watered environments. *Field Crops Research* **124**, 37–45.
- Mader A, Langer M, Knippers J, Speck O.** 2020. Learning from plant movements triggered by bulliform cells: the biomimetic cellular actuator. *Journal of the Royal Society Interface* **17**, 20200358.
- Matschi S, Vasquez MF, Bourgault R, Steinbach P, Chamness J, Kaczmar N, Gore MA, Molina I, Smith LG.** 2020. Structure-function analysis of the maize bulliform cell cuticle and its potential role in dehydration and leaf rolling. *Plant Direct* **4**, e00282.
- McAdam SA, Brodribb TJ.** 2016. Linking turgor with ABA biosynthesis: implications for stomatal responses to vapor pressure deficit across land plants. *Plant Physiology* **171**, 2008–2016.
- McDowell N, Pockman WT, Allen CD, et al.** 2008. Mechanisms of plant survival and mortality during drought: why do some plants survive while others succumb to drought? *New Phytologist* **178**, 719–739.
- Muggeo VMR.** 2008. Segmented: an R package to fit regression models with broken-line relationships. *R News* **8**, 20–25.
- Nardini A, Tyree MT, Salleo S.** 2001. Xylem cavitation in the leaf of *Prunus laurocerasus* and its impact on leaf hydraulics. *Plant Physiology* **125**, 1700–1709.
- O'Toole JC, Cruz RT, Singh TN.** 1979. Leaf rolling and transpiration. *Plant Science Letters* **16**, 111–114.
- Price AH, Young EM, Tomos AD.** 1997. Quantitative trait loci associated with stomatal conductance, leaf rolling and heading date mapped in upland rice (*Oryza sativa*). *New Phytologist* **137**, 83–91.
- Rodriguez-Dominguez CM, Buckley TN, Egea G, de Cires A, Hernandez-Santana V, Martorell S, Diaz-Espejo A.** 2016. Most stomatal closure in woody species under moderate drought can be explained by stomatal responses to leaf turgor. *Plant, Cell & Environment* **39**, 2014–2026.
- Sack L, Scoffoni C.** 2012. Measurement of leaf hydraulic conductance and stomatal conductance and their responses to irradiance and dehydration using the evaporative flux method (EFM). *Journal of Visualized Experiments* **70**, e4179.
- Saglam A, Kadioglu A, Demiralay M, Terzi R.** 2014. Leaf rolling reduces photosynthetic loss in maize under severe drought. *Acta Botanica Croatica* **73**, 315–332.
- Salmon Y, Lintunen A, Dayet A, Chan T, Dewar R, Vesala T, Holttä T.** 2020. Leaf carbon and water status control stomatal and nonstomatal limitations of photosynthesis in trees. *New Phytologist* **226**, 690–703.
- Salvi AM, Smith DD, Adams MA, McCulloh KA, Givnish TJ.** 2021. Mesophyll photosynthetic sensitivity to leaf water potential in *Eucalyptus*: a new dimension of plant adaptation to native moisture supply. *New Phytologist* **230**, 1844–1855.
- Scoffoni C, Rawls M, McKown A, Cochard H, Sack L.** 2011. Decline of leaf hydraulic conductance with dehydration: relationship to leaf size and venation architecture. *Plant Physiology* **156**, 832–843.
- Scoffoni C, Vuong C, Diep S, Cochard H, Sack L.** 2014. Leaf shrinkage with dehydration: coordination with hydraulic vulnerability and drought tolerance. *Plant Physiology* **164**, 1772–1788.

- Sevanto S, McDowell NG, Dickman LT, Pangle R, Pockman WT.** 2014. How do trees die? A test of the hydraulic failure and carbon starvation hypotheses. *Plant, Cell & Environment* **37**, 153–161.
- Sirault XR, Condon AG, Wood JT, Farquhar GD, Rebetzke GJ.** 2015. ‘Rolled-upness’: phenotyping leaf rolling in cereals using computer vision and functional data analysis approaches. *Plant Methods* **11**, 52.
- Smith-Martin CM, Skelton RP, Johnson KM, Lucani C, Brodribb TJ, Sala A.** 2020. Lack of vulnerability segmentation among woody species in a diverse dry sclerophyll woodland community. *Functional Ecology* **34**, 777–787.
- Sorek Y, Greenstein S, Netzer Y, Shtein I, Jansen S, Hochberg U.** 2021. An increase in xylem embolism resistance of grapevine leaves during the growing season is coordinated with stomatal regulation, turgor loss point and intervessel pit membranes. *New Phytologist* **229**, 1955–1969.
- Souza RP, Machado EC, Silva JAB, Lagôa AMMA, Silveira JAG.** 2004. Photosynthetic gas exchange, chlorophyll fluorescence and some associated metabolic changes in cowpea (*Vigna unguiculata*) during water stress and recovery. *Environmental and Experimental Botany* **51**, 45–56.
- Tombesi S, Nardini A, Frioni T, Soccolini M, Zadra C, Farinelli D, Poni S, Palliotti A.** 2015. Stomatal closure is induced by hydraulic signals and maintained by ABA in drought-stressed grapevine. *Scientific Reports* **5**, 12449.
- Trueba S, Pan R, Scoffoni C, John GP, Davis SD, Sack L.** 2019. Thresholds for leaf damage due to dehydration: declines of hydraulic function, stomatal conductance and cellular integrity precede those for photochemistry. *New Phytologist* **223**, 134–149.
- Tyree MT, Sperry JS.** 1989. Vulnerability of xylem to cavitation and embolism. *Annual Review of Plant Physiology and Plant Molecular Biology* **40**, 19–36.
- Wang X, Du T, Huang J, Peng S, Xiong D.** 2018. Leaf hydraulic vulnerability triggers the decline in stomatal and mesophyll conductance during drought in rice (*Oryza sativa*). *Journal of Experimental Botany* **69**, 4033–4045.
- Wang X, Zhao J, Huang J, Peng S, Xiong D.** 2022. Evaporative flux method of leaf hydraulic conductance estimation: sources of uncertainty and reporting format recommendation. *Plant Methods* **18**, 63.
- Wong SC, Canny MJ, Holloway-Phillips M, Stuart-Williams H, Cernusak LA, Marquez DA, Farquhar GD.** 2022. Humidity gradients in the air spaces of leaves. *Nature Plants* **8**, 971–978.
- Yang S, Tyree MT.** 1993. Hydraulic resistance in *Acer saccharum* shoots and its influence on leaf water potential and transpiration. *Tree Physiology* **12**, 231–242.
- Yang W, Feng H, Zhang X, Zhang J, Doonan JH, Batchelor WD, Xiong L, Yan J.** 2020. Crop phenomics and high-throughput phenotyping: past decades, current challenges, and future perspectives. *Molecular Plant* **13**, 187–214.
- Yao G, Nie Z, Turner N, Li F, Gao T, Fang X, Scoffoni C.** 2021. Combined high leaf hydraulic safety and efficiency provides drought tolerance in *Caragana* species adapted to low mean annual precipitation. *New Phytologist* **229**, 230–244.
- Zhu S, Chen Y, Ye Q, He P, Liu H, Li R, Fu P, Jiang G, Cao K.** 2018. Leaf turgor loss point is correlated with drought tolerance and leaf carbon economics traits. *Tree Physiology* **38**, 658–663.